

Physico-Chemical and Electrical Properties of Bismuth Chromate Solid Solutions

Wong Y. C.^{1,2} and Tan Y. P.^{1,2*}

¹Centre of Excellence for Catalysis Science and Technology, Universiti Putra Malaysia, 43400 Serdang, Selangor, Malaysia

²Department of Chemistry, Faculty of Science, Universiti Putra Malaysia, 43400 Serdang, Selangor, Malaysia

ABSTRACT

Bismuth chromium solid solutions, with a general formula $\text{Bi}_{6-x}\text{Cr}_2\text{O}_8$, where $-1 \leq x \leq 2$, were successfully synthesized via the conventional solid state method. The phases of the synthesized samples were determined by X-ray diffraction (XRD) analysis. The properties of single-phase compounds were characterized by using differential thermal analysis (DTA), thermal gravimetric analysis (TGA), AC impedance spectroscopy, and inductively coupled plasma-atomic emission spectroscopy (ICP-AES). The occurrence of phase transitions was confirmed by DTA and TGA, where a thermal event was observed by DTA at around 800°C. In addition, TGA studies also showed that there was a weight loss at around 800°C. Elemental analysis of $\text{Bi}_6\text{Cr}_2\text{O}_{15}$ and its solid solutions by ICP-AES showed a good agreement between the expected value and the experimental value on the compositions, with no evidence of any systematic deviation from stoichiometric. Electrical properties of $\text{Bi}_6\text{Cr}_2\text{O}_{15}$ and its solid solutions were investigated by using AC impedance spectroscopy from 300°C to 650°C. Ionic conductivity increased with the increasing temperature and bismuth content, and the best ionic conductivity was observed for $\text{Bi}_7\text{Cr}_2\text{O}_{16.5}$. The activation energy (E_a) of $\text{Bi}_6\text{Cr}_2\text{O}_{15}$ and its solid solutions were in the range of 1.22-1.32 eV.

Keywords: Bismuth oxide, Chromium oxide, Impedance spectroscopy

Article history:

Received: 18 May 2011

Accepted: 21 December 2011

E-mail addresses:

stevenwongyc@hotmail.com (Wong Y. C.),

yptan@science.upm.edu.my (Tan Y. P.),

*Corresponding Author

INTRODUCTION

Magneto-electric materials, in which magnetic and ferroelectric orders coexist, are currently attracting more and more attention owing to their potential applications and intriguing physics. Bi-based 3d-transition metal oxides with distorted perovskite structures, such as BiMnO_3 and BiFeO_3 , are important magneto-

electric materials (Chi *et al.*, 2007; Li *et al.*, 2006; Selbach *et al.*, 2010; Yang *et al.*, 2007). It is believed that the lone-pair electrons of Bi play a crucial role in ferroelectricity. The $\text{Bi}_2\text{O}_3\text{-Cr}_2\text{O}_3$ system was investigated to explore novel magneto-electric compounds.

The phase diagram of the $\text{Bi}_2\text{O}_3\text{-Cr}_2\text{O}_3$ system consisted of three compounds which were synthesized by solid-state reactions: $\text{Bi}_{18}\text{CrO}_{30}$ (tetragonal, $a = b = 7.74 \text{ \AA}$, $c = 5.72 \text{ \AA}$), $\text{Bi}_6\text{Cr}_2\text{O}_{15}$ (orthorhombic, $a = 5.55 \text{ \AA}$, $b = 5.76 \text{ \AA}$, $c = 5.50 \text{ \AA}$), and BiCrO_3 (orthorhombic, $a = 10.52 \text{ \AA}$, $b = 17.63 \text{ \AA}$, $c = 9.995 \text{ \AA}$) (Liu *et al.*, 2008). Later, the phase diagram of the pseudo-binary system $\text{Bi}_2\text{O}_3\text{-Cr}_2\text{O}_3$ was reconstructed based on the x-ray diffraction measurement and differential thermal analysis by Liu *et al.* (2008). Four intermediate phases were determined in this system, namely, $\text{Bi}_{14}\text{CrO}_{24}$ -based solid solutions (space group I4Im), $\text{Bi}_{10}\text{Cr}_2\text{O}_{21}$ -based high temperature solid solutions (orthorhombic symmetry), a new compound Bi_2CrO_6 (monoclinic symmetry) and the stoichiometric compound $\text{Bi}_6\text{Cr}_2\text{O}_{15}$ (orthorhombic symmetry, with unit cell parameters, $a = 12.3018 \text{ \AA}$, $b = 19.8749 \text{ \AA}$, and $c = 5.8816 \text{ \AA}$ and space group Ccc2) (Liu *et al.*, 2008).

In term of ionic conductivity, the compound $\text{Bi}_6\text{Cr}_2\text{O}_{15}$ could be expected to be a good oxygen ion conductor, in view of its structural similarity to the solid solution $\text{Bi}(\text{Bi}_{12-x}\text{Te}_x\text{O}_{14})\text{Mo}_{4-x}\text{V}_{1+x}\text{O}_{20}$ ($0 \leq x \leq 2.5$), which exhibits a conductivity as high as $\sigma = 8.0 \times 10^{-3} (\Omega \text{ cm})^{-1}$ at 750°C ($x = 1$) with an activation energy, $E_a = 0.84 \text{ eV}$. It is, however, found to be considerably modest oxygen ion conductor. It is speculative to attribute this to any structural difference between the phases, but it seems to imply that the high oxygen ion mobility in the column phases is not provided solely by the presence of the column, but also significantly depends on the atoms and the arrangement between the columns (Grins *et al.*, 2002).

Previously, the thermogravimetric analyses done by Esmaeilzadeh *et al.* (2001) showed that upon heating mixtures of Bi_2O_3 and Cr_2O_3 in air, an irreversible increase in weight began at $450\text{-}500^\circ\text{C}$ and reached, depending on the Cr concentration, a plateau at $650\text{ to }900^\circ\text{C}$. The weight increase corresponded well to that of a complete oxidation of Cr^{3+} to Cr^{6+} . This oxidative behaviour is quite unusual for Cr-containing materials in air, at normal pressure, and these high temperatures. Magnetic susceptibility measurements confirmed an oxidation state of $+6$ for Cr, as no or only very weak paramagnetic signals were observed (Colmont *et al.*, 2010).

In this work, the focus was placed on synthesizing $\text{Bi}_6\text{Cr}_2\text{O}_{15}$ and its solid solutions, as well as investigating their physico-chemical and electrical properties.

EXPERIMENTAL

Powder sample of bismuth chromate ($\text{Bi}_6\text{Cr}_2\text{O}_{15}$) and its solid solutions were prepared via solid state reactions using Bi_2O_3 (Aldrich, 99.999%) and Cr_2O_3 [Johnson Matthey (JM), 99.999%] as starting materials. The samples were heat-treated at 600°C for 48-72 hours with intermediate grindings. The phase identity and purity of the synthesized samples were determined by X-ray diffraction (XRD) analysis (Shimadzu diffractometer XRD-6000), which was equipped with a diffracted-beam graphite monochromator using $\text{CuK}\alpha$ radiation. The morphology of the samples was studied using scanning electron microscopy (LEO 1455 VP SEM).

The thermal properties of the samples were determined by using the differential thermal analysis, DTA (Perkin-Elmer instrument, model DTA 7) and thermal gravimetric analysis, TGA (Mettler Toledo Star SW 7.01). Inductively coupled plasma-atomic emission spectroscopy (ICP-

AES) (Perkin-Elmer P1000) was used to carry out the elemental analysis. Fourier-transform infrared (FT-IR) spectrometer (Perkin-Elmer model 1725x), with the wavenumber range in the region of 4000 and 400 cm^{-1} , was used for the structural analysis. The electrical properties of the pelleted samples were studied by using AC impedance analyzer (Hewlett-Packard Impedance Analyzer HP 4192A). The frequency range of 5 Hz to 13 MHz with an applied voltage of 100 mV was used. The measurements were made between 300°C and 650°C by increment steps of 50°C with 30 minutes stabilization time. The measurements were carried out on heat-cool thermal cycles.

RESULTS AND DISCUSSION

XRD and SEM Results

Fig.1 shows the XRD pattern of $\text{Bi}_6\text{Cr}_2\text{O}_{15}$ and its solid solutions prepared via conventional solid state method. $\text{Bi}_6\text{Cr}_2\text{O}_{15}$ and its solid solutions were indexed using the orthorhombic system with lattice parameters: $a = 12.30184 \text{ \AA}$, $b = 19.87492 \text{ \AA}$, $c = 5.88162 \text{ \AA}$, and in space group of Ccc2 (Grins *et al.*, 2002; Liu *et al.*, 2008). From the results obtained, the limit of the solid solutions in Bi_2O_3 - Cr_2O_3 system was in the range 4 to 7. The four single phase solid solutions that crystallized in orthorhombic system were $\text{Bi}_4\text{Cr}_2\text{O}_{12}$, $\text{Bi}_5\text{Cr}_2\text{O}_{13.5}$, $\text{Bi}_6\text{Cr}_2\text{O}_{15}$ and $\text{Bi}_7\text{Cr}_2\text{O}_{16.5}$. As for $\text{Bi}_3\text{Cr}_2\text{O}_{10.5}$, two extra peaks were observed at 24.5 ° and 33.6°. These two peaks were due to the formation of chromium oxide (ICDD card number, 01-070-3765). Meanwhile, there were seven extra peaks observed in $\text{Bi}_8\text{Cr}_2\text{O}_{18}$, in the positions of 31.0778 °, 32.6381 °, 45.4703 °, 46.5948 °, 53.2193 °, 54.6160 °, and 55.2515 °. All these peaks were attributed to the formation of δ -bismuth oxide (δ - Bi_2O_3) (ICDD card number: 01-074-1633, 00-027-0052, 00-051-1161).

As the composition varies, the solid solutions may undergo a small contraction or expansion. According to Vegard's law, unit-cell parameters should change linearly with the composition. The evolution of the unit-cell parameters versus composition was plotted and is shown in Fig.2 to Fig.4. All the parameters a , b and c underwent a regular increase from $x = 4$ to $x = 7$. This general increase of all unit-cell parameters can be expected, since a smaller cation, Cr (ionic radius = 0.51 Å), is being substituted for by a larger Bi (ionic radius = 1.20 Å) (Bégué *et al.*, 2002).

Fig.5(a), (b), (c), and (d) show the scanning electron microscopy (SEM) images of the samples. All the samples have displayed a similar morphology where the microstructures were homogeneously distributed in the lattice. No secondary phase was observed in the structure, and therefore, the samples synthesized were in the single phase. Some pores were also observed in the inter-granular area, indicating a moderate connection between the grains.

Structural Analysis

The IR absorption spectra of the single-phase orthorhombic structure compounds, $\text{Bi}_x\text{Cr}_2\text{O}_8$, $4 \leq x \leq 7$, have similar patterns as shown in Fig.6. A broad, diffuse band was observed at $\sim 850 \text{ cm}^{-1}$ and $\sim 792 \text{ cm}^{-1}$ in the IR spectra of all the compounds. This may be due to the Cr-O-Cr bond vibration and Cr-O stretching (Brown *et al.*, 1967; Jezowska-Trzebiatowska *et al.*, 1968).

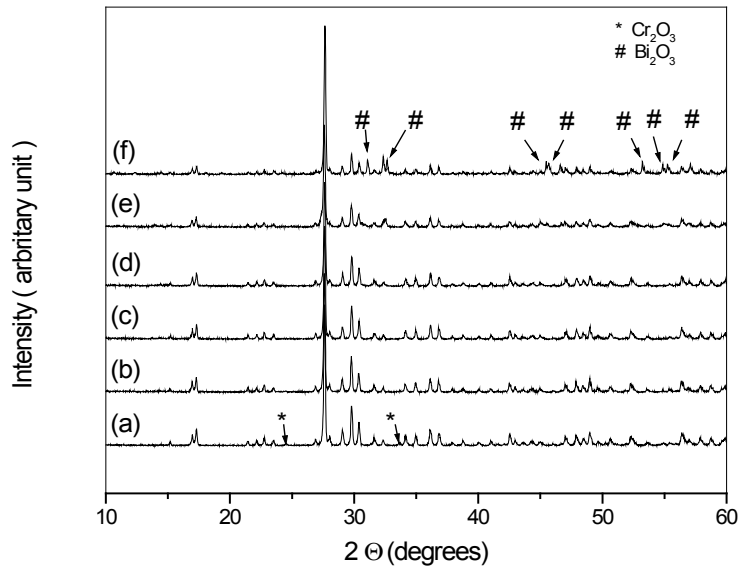


Fig. 1: The XRD patterns of (a) $\text{Bi}_3\text{Cr}_2\text{O}_{10.5}$, (b) $\text{Bi}_4\text{Cr}_2\text{O}_{12}$, (c) $\text{Bi}_5\text{Cr}_2\text{O}_{13.5}$, (d) $\text{Bi}_6\text{Cr}_2\text{O}_{15}$, (e) $\text{Bi}_7\text{Cr}_2\text{O}_{16.5}$, and (f) $\text{Bi}_8\text{Cr}_2\text{O}_{18}$ prepared at 600°C

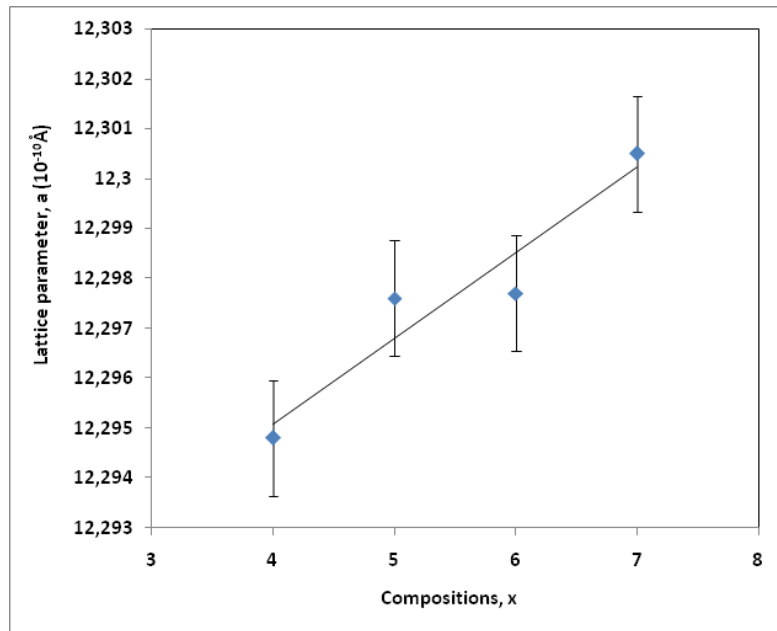


Fig.2: Variation of the lattice parameter, a , with composition, x , in $\text{Bi}_x\text{Cr}_2\text{O}_8$, $4 \leq x \leq 7$

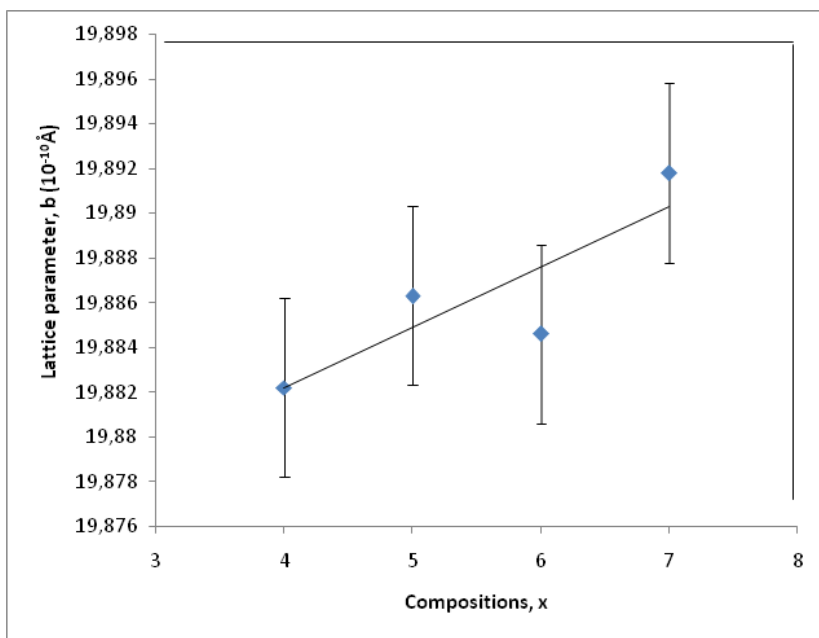


Fig.3: Variation of the lattice parameter, b , with composition, x , in $\text{Bi}_x\text{Cr}_2\text{O}_8$, $4 \leq x \leq 7$

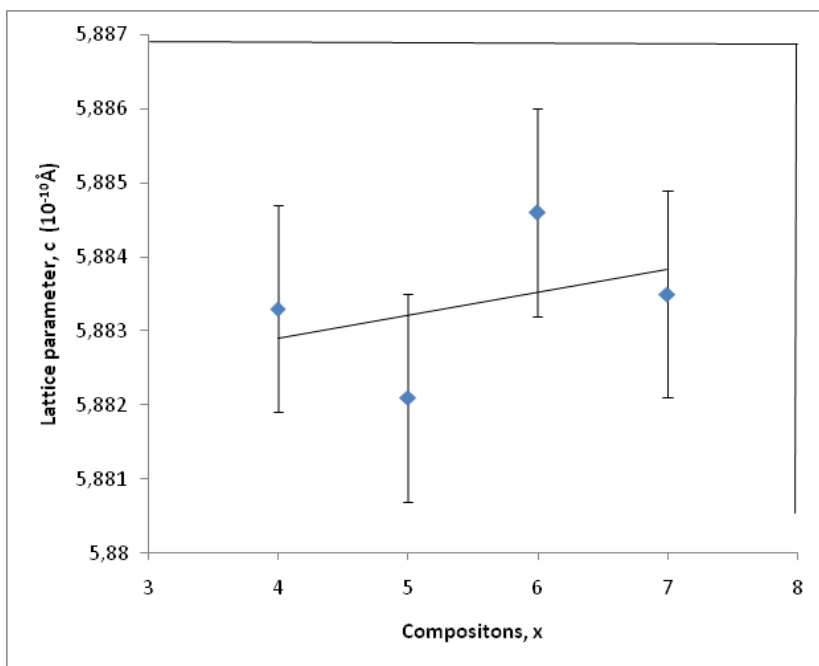


Fig.4: Variation of the lattice parameter, c , with composition, x , in $\text{Bi}_x\text{Cr}_2\text{O}_8$, $4 \leq x \leq 7$

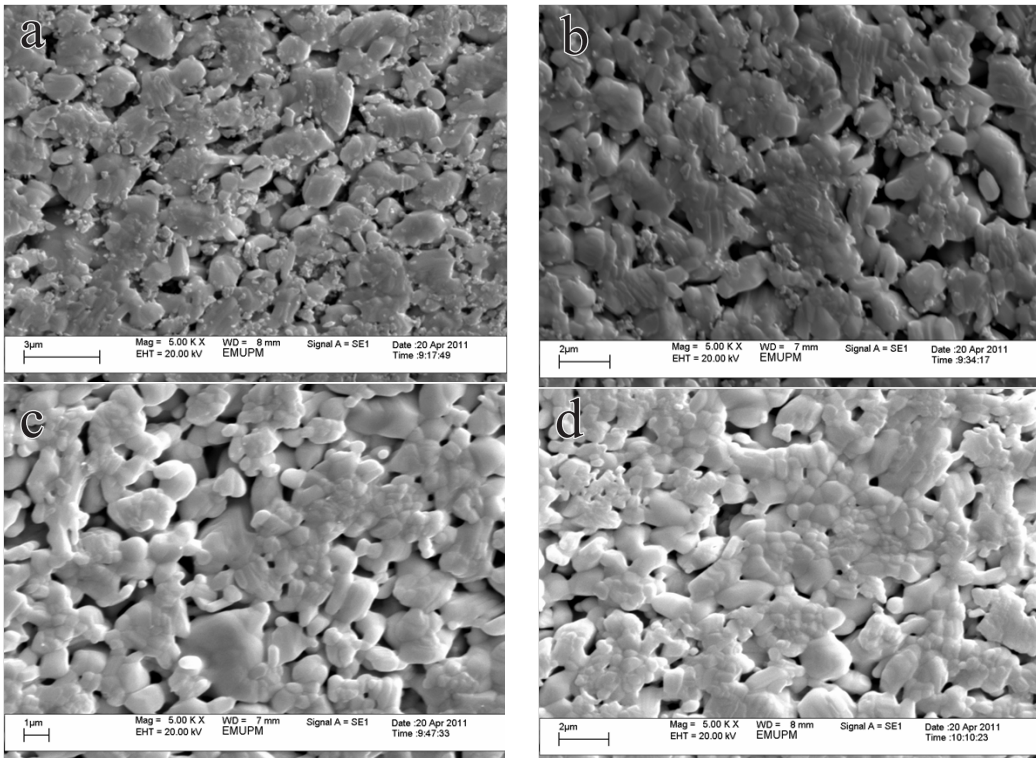


Fig.5: The SEM image for (a) $\text{Bi}_4\text{Cr}_2\text{O}_{12}$, (b) $\text{Bi}_5\text{Cr}_2\text{O}_{13.5}$, (c) $\text{Bi}_6\text{Cr}_2\text{O}_{15}$, and (d) $\text{Bi}_7\text{Cr}_2\text{O}_{16.5}$, sintered at 600°C

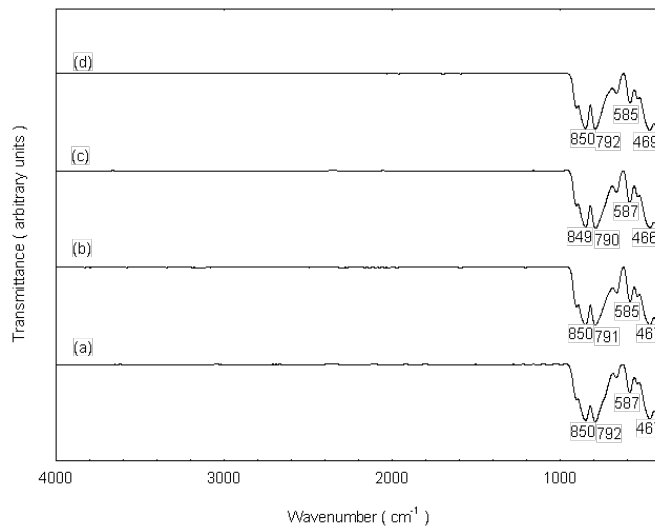
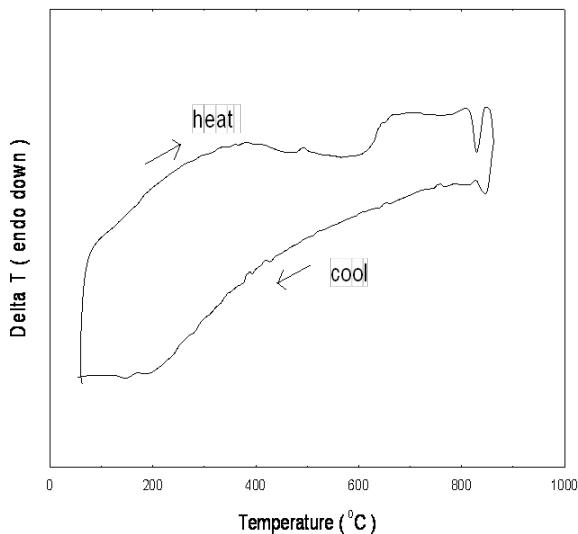
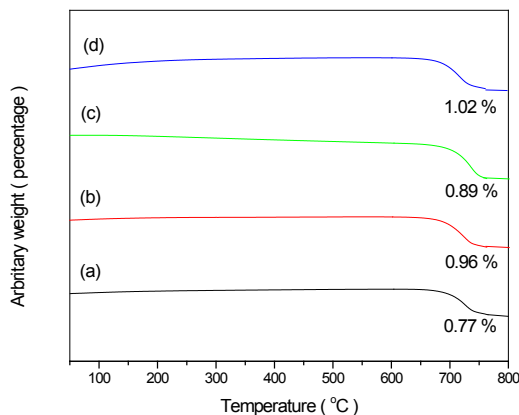


Fig.6: The FT-IR spectra of (a) $\text{Bi}_4\text{Cr}_2\text{O}_{12}$, (b) $\text{Bi}_5\text{Cr}_2\text{O}_{13.5}$, (c) $\text{Bi}_6\text{Cr}_2\text{O}_{15}$, and (d) $\text{Bi}_7\text{Cr}_2\text{O}_{16.5}$

Fig.7: DTA thermogram of $\text{Bi}_6\text{Cr}_2\text{O}_{15}$ Fig.8: The TGA thermographs of (a) $\text{Bi}_4\text{Cr}_2\text{O}_{12}$, (b) $\text{Bi}_5\text{Cr}_2\text{O}_{13.5}$, (c) $\text{Bi}_6\text{Cr}_2\text{O}_{15}$, and (d) $\text{Bi}_7\text{Cr}_2\text{O}_{16.5}$ with their respective percentage weight loss

However, no shift was observed in the wavenumbers of Cr-O-Cr bond vibration, as well as Cr-O stretching with the variation of the Cr content. The band of $\sim 587\text{ cm}^{-1}$ and $\sim 467\text{ cm}^{-1}$ in the IR spectra was attributed to the vibration of Bi-O and Bi-O-Bi vibrations of $[\text{BiO}_6]$ octahedral units, respectively (Cheng *et al.*, 2006; Rico-Fuentes *et al.*, 2005).

The atomic weight of Bi is about four times larger than that of Cr. Moreover, the ionic radius of Bi^{3+} (1.20 \AA) is larger than that of Cr^{3+} (0.69 \AA). Thus, Bi-O bond length is expected to be longer and weaker compared to Cr-O bond. This may lead to the lowering of wavenumber (ν) at 587 cm^{-1} and 467 cm^{-1} . The Bi contents for the compounds $\text{Bi}_x\text{Cr}_2\text{O}_6$, $4 \leq x \leq 7$ are different and it is expected that ν would decrease with increasing Bi content. However, from the IR spectra obtained, the ν does not decrease with the increasing Bi content. It may be due to Bi-O

bond existed in the form of $[\text{BiO}_6]$ octahedral units which restricted its vibration (Ardelean *et al.*, 2008).

Thermal Properties

The DTA thermograms of all solid solutions exhibited a similar pattern. Here, only the thermogram of $\text{Bi}_6\text{Cr}_2\text{O}_{15}$ (Fig. 7) is shown for discussion. The endothermic peak around 600°C was due to the oxidation of Cr^{3+} into Cr^{6+} , which began at 450°C to 600°C (Esmailzadeh *et al.*, 2001). Besides, an endothermic peak was also observed at the temperature around 800°C on the heating cycle, which ascribed to the transformation of orthorhombic $\text{Bi}_6\text{Cr}_2\text{O}_{15}$ into the high temperature solid solution, face-centred orthorhombic $\text{Bi}_{10}\text{Cr}_2\text{O}_{21}$. It was an irreversible transformation, where the face-centred orthorhombic $\text{Bi}_{10}\text{Cr}_2\text{O}_{21}$, once formed at 800°C , could not be transformed back into the orthorhombic $\text{Bi}_6\text{Cr}_2\text{O}_{15}$ on cooling (Liu *et al.*, 2008).

All the solid solutions showed a similar TGA thermograph pattern (Fig. 8). In particular, Thermogravimetric measurements did not show any weight loss when the samples were heated up until 700°C . After 700°C , a weight loss was observed, indicating $\text{Bi}_6\text{Cr}_2\text{O}_{15}$ and its solid solutions had undergone phase transition from orthorhombic to face-centred orthorhombic structure (Liu *et al.*, 2008). It further confirmed the DTA results that the phase transition occurred at high temperature.

Elemental Analysis

The compositions of the solid solutions were examined by using ICP-AES and the data are shown in Table 1. With the increasing chromium content in the order of $\text{Bi}_7\text{Cr}_2\text{O}_{16.5}$ to $\text{Bi}_4\text{Cr}_2\text{O}_{12}$, both $\text{Bi}_4\text{Cr}_2\text{O}_{12}$ and $\text{Bi}_5\text{Cr}_2\text{O}_{13.5}$ were unable to dissolve either in concentrated hydrochloric acid (HCl) or hydrofluoric acid (HF). Therefore, the elemental analysis for the chromium content in these two samples was ignored. These two samples were tested only for bismuth composition. In general, the experimental values for the composition are in good agreement with the calculated values, with no evidence of any systematic deviation from the stoichiometric. Thus, the stoichiometric compositions of the single phase materials were confirmed.

TABLE 1: Composition determination of solid solutions in the $\text{Bi}_2\text{O}_3\text{-Cr}_2\text{O}_3$ system

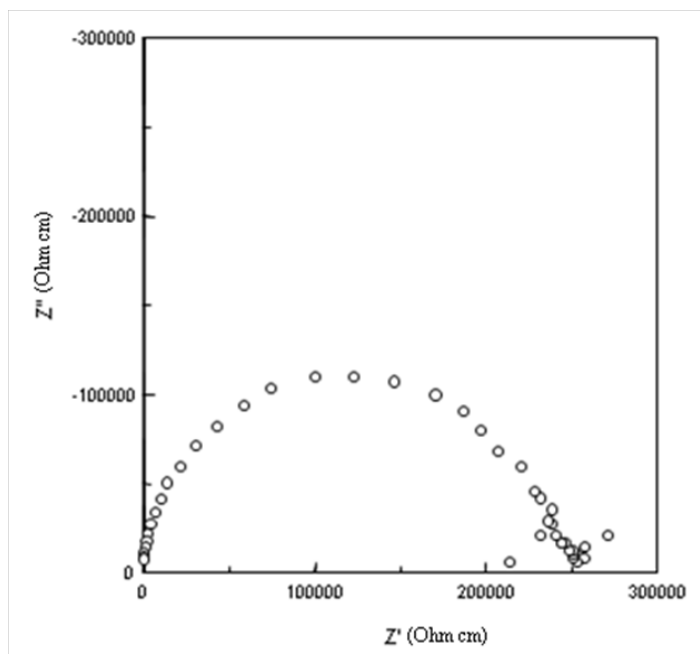
Sample	Elements	Atomic %	
		Calculated	Experimental
$\text{Bi}_4\text{Cr}_2\text{O}_{12}$	Bi	73.85	76.78 ± 0.56
	Cr	-	-
	O	-	-
$\text{Bi}_5\text{Cr}_2\text{O}_{13.5}$	Bi	76.56	76.57 ± 0.60
	Cr	-	-
	O	-	-

TABLE 1: (continued)

Bi ₆ Cr ₂ O ₁₅	Bi	78.47	78.70 ± 0.19
	Cr	6.51	6.34 ± 0.48
	O	15.02	14.96
Bi ₇ Cr ₂ O _{16.5}	Bi	79.90	81.93 ± 0.72
	Cr	5.68	5.54 ± 0.61
	O	14.42	12.53

Electrical Properties

The conductivity values of the materials were extracted from complex plane plots. In general, the complex plane plots of the four solid solutions were similar, and therefore, the parent compound (Bi₆Cr₂O₁₅) was selected for the discussion. The conductivity measurements of solid solutions were reproducible on heating and cooling. The complex plane plot of Bi₆Cr₂O₁₅ at 450°C (Fig.9) showed that the resistance (R) of the material was 2.3871×10^5 ohm cm. Thus, the semicircle has an associated capacitance (C_b) (calculated from $\omega RC = 1$, where ω is the frequency of maximum loss) of 6.67×10^{-12} F cm⁻¹, which is a typical value for bulk component. The conductivity of the material at 450°C was 4.189×10^{-6} Ω⁻¹ cm⁻¹. The moderate ionic conductivity of the samples was due to the moderate connection between the grains, as a result of the presence of pore in the inter-granular area, as shown in the SEM image (Fig.5). As the temperature increased, the intercept at the real component of impedance, Z' (resistive) axis shifted towards lower value and gave the lower resistance value. Hence, the conductivity


 Fig.9: A complex plane plot of Bi₆Cr₂O₁₅ at 450°C

increased with the increasing temperature. The optimum conductivity of $\text{Bi}_6\text{Cr}_2\text{O}_{15}$ was observed at 650°C with a conductivity value of $4.456 \times 10^{-4} \Omega^{-1} \text{cm}^{-1}$.

The homogeneity of the materials can be observed from the complex plane plots. A single semicircle observed indicated that this material was homogeneous. The homogeneity of the materials can also be determined from the combined spectroscopic plots of electric modulus, M'' , and the imaginary components of impedance, $-Z''$ versus $\log f$ (where f was frequency). Fig.10 shows the combined spectroscopic plots of M'' , $-Z''$ versus $\log f$ of $\text{Bi}_6\text{Cr}_2\text{O}_{15}$ at 450°C . It showed a single peak and the frequency maxima of Z'' and M'' coincided at a higher frequency, where the full width at half maximum (FWHM) of the Z'' peaks was approximately 1.4 decade. Thus, this material can be considered as homogeneous and the conductivity was purely attributed by bulk.

Ionic conductivity is temperature dependence and is related by the Arrhenius equation:

$$\sigma = A \exp(-E / RT) \quad (1)$$

where σ is ionic conductivity, A is pre-exponential factor, E is activation energy, R is constant and T is temperature. When the temperature increases, the mobility of ions also increases and thus the ionic conductivity increases.

Fig.11 shows the combination of the Arrhenius plots of all pure phase solid solutions in $\text{Bi}_2\text{O}_3\text{-Cr}_2\text{O}_3$ system. The conductivity behaviour is similar for all materials studied and is temperature dependence. The conductivity increased in the order of $\text{Bi}_4\text{Cr}_2\text{O}_{12} < \text{Bi}_5\text{Cr}_2\text{O}_{13.5} \sim \text{Bi}_6\text{Cr}_2\text{O}_{15} < \text{Bi}_7\text{Cr}_2\text{O}_{16.5}$. The conductivity increased with the increasing bismuth content in the stoichiometric equation. Meanwhile, the ionic radius of bismuth is larger than chromium, and therefore enlarging the cell volume of the materials and making the passage of charge carriers through more feasible cells (Galy *et al.*, 2003).

A linear straight line was observed from 400°C up to 650°C . Below 400°C , a curvature was observed. The curvature in the plot may be due to a temperature dependence of the activation energy (e.g., $E_a = E_{a0} - E_{a1}.T^2$) or to different conduction mechanisms dominating at lower and higher temperatures (Grins *et al.*, 2002). Deviation at high temperature can correlate to the phase transformation from $\text{Bi}_6\text{Cr}_2\text{O}_{15}$ to face-centred orthorhombic $\text{Bi}_{10}\text{Cr}_2\text{O}_{21}$ and monoclinic Bi_2CrO_6 above 650°C (Liu *et al.*, 2008). From the linear range of the plot, the activation energies (E_a) calculated were in the range within 1.22 eV to 1.32 eV. The best ionic solid has an activation energy of 1 eV (96 kJ mole^{-1}) or lower. For example, $\text{Bi}_5\text{NbO}_{10}$ and $\text{Bi}_{26}\text{Mo}_{10}\text{O}_8$, which are good ionic conductors, have E_a of 0.94 eV and 0.47 eV, respectively (Hou *et al.*, 2010; Begue *et al.*, 1998). Hence, solid solutions in $\text{Bi}_2\text{O}_3\text{-Cr}_2\text{O}_3$ system were considered as moderate oxide ion conductors.

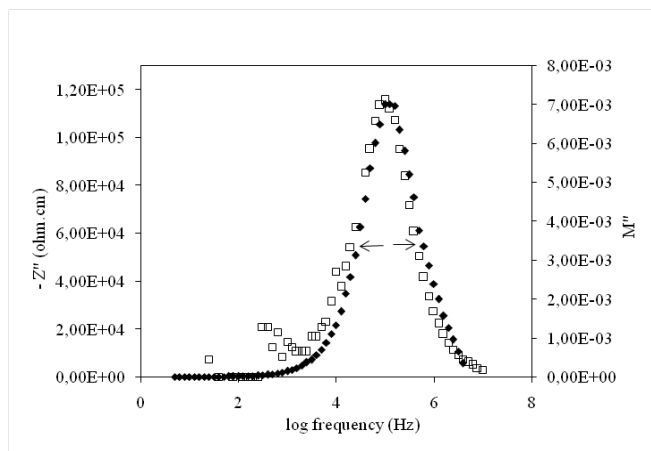


Fig.10: The modulus spectroscopic plot of M'' , $-Z''$ versus $\log f$ of $\text{Bi}_6\text{Cr}_2\text{O}_{15}$ at 450°C

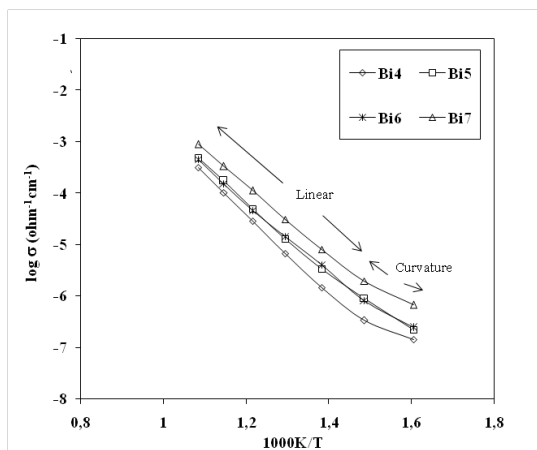


Fig.11: The Arrhenius conductivity plots of $\text{Bi}_x\text{Cr}_2\text{O}_8$ ($4 \leq x \leq 7$)

CONCLUSION

The solid solutions in the $\text{Bi}_2\text{O}_3 - \text{Cr}_2\text{O}_3$ system have been successfully synthesized via conventional solid state method. Among the compounds synthesized in which Bi:Cr ratio range from 1.5:1 to 4:1 and as determined from the X-ray diffraction (XRD) analyses, only four were in the pure phase with the orthorhombic structure, i.e. $\text{Bi}_4\text{Cr}_2\text{O}_{12}$, $\text{Bi}_5\text{Cr}_2\text{O}_{13.5}$, $\text{Bi}_6\text{Cr}_2\text{O}_{15}$ and $\text{Bi}_7\text{Cr}_2\text{O}_{16.5}$. The SEM image showed a homogeneous dispersion of microstructure and the presence of pores in the inter-granular area. The occurrence of the phase transitions at high temperatures was confirmed by the thermal analyses. The thermal analyses showed an irreversible endothermic peak at temperature $\sim 800^\circ\text{C}$ on heating cycle. Besides, the TGA results showed that there is a weight loss after 700°C .

The activation energy for the solid solution in $\text{Bi}_2\text{O}_3\text{-Cr}_2\text{O}_3$ system is in the range 1.22 eV- 1.32 eV. The moderate ionic conductivity of the samples can be related to the moderate

connection between the grains, which is due to the presence of pores in the inter-granular area. However, conductivity increases with the increasing temperature and bismuth content. The conductivity of the solid solutions increased in the order of: $\text{Bi}_4\text{Cr}_2\text{O}_{12} < \text{Bi}_5\text{Cr}_2\text{O}_{13.5} \sim \text{Bi}_6\text{Cr}_2\text{O}_{15} < \text{Bi}_7\text{Cr}_2\text{O}_{16.5}$. Among the solid solutions, $\text{Bi}_7\text{Cr}_2\text{O}_{16.5}$ is the best ionic conductor and has the highest conductivity. From the results of the electrical measurement, the solid solutions for Bi_2O_3 - Cr_2O_3 system can be concluded as moderate oxide ion conductors at the temperature above 350°C.

ACKNOWLEDGEMENTS

The authors are grateful for the financial support given by the Ministry of Science, Technology, and Innovation (MOSTI) via Science Fund.

REFERENCES

- Ardelean, I., Cora, S., & Rusu, D. (2008). EPR and FT-IR spectroscopic studies of Bi_2O_3 - B_2O_3 -CuO glasses. *Physica B*, 403, 3682–3685.
- Begue, P., Rojo, J. M., Enjalbert, R., Galy, J., & Castro, A. (1998). Ionic conductivity of the new oxide family $\text{Bi}[\text{Bi}_{12-x}\text{Te}_x\text{O}_{14}]\text{Mo}_{4-x}\text{V}_{1+x}\text{O}_{20}$. *Solid State Ionics*, 112, 275–280.
- Bëguë, P., Rojo, J.M., Iglesias, J. E., & Castro, A. (2002). Different $[\text{Bi}_{12}\text{O}_{14}]_n$ columnar structural types in the Bi-Mo-Cr-O system: synthesis, structure, and electrical properties of the solid solution $\text{Bi}_{26}\text{Mo}_{10-x}\text{Cr}_x\text{O}_{69}$. *Journal of Solid State Chemistry*, 166, 7-14.
- Brown, D. A., Cunningham, D., & Glass, W. K. (1967). The infrared and Raman spectra of chromium (III) oxide. *Spectrochimica Acta Part A: Molecular Spectroscopy*, 24, 965- 968.
- Cheng, Y., Xiao, H. N., Guo, W. M., & Guo, W. M. (2006). Structure and crystallization kinetics of Bi_2O_3 - B_2O_3 glasses. *Thermochimica Acta*, 444, 173–178.
- Chi, Z. H., Yang, H., Feng, S. M., Li, F. Y., Yu, R. C., & Jin, C. Q. (2007). Room-temperature ferroelectric polarization in multiferroic BiMnO_3 . *Journal of Magnetism and Magnetic Materials*, 310, e358-e360.
- Colmont, M., Drache, M., & Roussel, P. (2010). Synthesis and characterization of $\text{Bi}_{31}\text{Cr}_5\text{O}_{61.5}$, a new bismuth chromium oxide, potential mixed-ionic-electronic conductor for solid oxide fuel cells. *Journal of Power Sources*, 195, 7207-7212.
- Esmailzadeh, S., Lundgren, S., Haslenius, U., & Grins, J. (2001). $\text{Bi}_{1-x}\text{Cr}_x\text{O}_{1.5+1.5x}$, $0.05 \leq x \leq 0.15$: A new high-temperature solid solution with a three-dimensional incommensurate modulation. *Journal of Solid State Chemistry*, 156, 168-180.
- Galy, J., Enjalbert, R., Rozier, P., & Millet, P. (2003). Lone pair stereoactivity versus anionic conductivity. Columnar structures in the Bi_2O_3 - MoO_3 system. *Solid State Sciences*, 5, 165-174.
- Grins, J., Esmailzadeh, S., & Hull, S. (2002). Structure and ionic conductivity of $\text{Bi}_6\text{Cr}_2\text{O}_{15}$, a new structure type containing $(\text{Bi}_{12}\text{O}_{14})^{8n+}$ columns and CrO_4^{2-} tetrahedra. *Journal of Solid State Chemistry*, 163, 144–150.
- Hou, J. G., Vaisha, R., Qu, Y. F., Krsmanovic, D., Varma, K. B. R., & Kumar, R. V. (2010). Dielectric relaxation and electrical conductivity in $\text{Bi}_5\text{NbO}_{10}$ oxygen ion conductors prepared by a modified sol-gel process. *Journal of Power Source*, 195, 2613-2618.

- Jezowska-Trzebiatowska, B., Hanuza, J., Wojciechowski, W., & Nawojkska, J. (1968). Spectroscopic studies and structural chemistry of Cr^{III}/Cr^{VI} compounds in the solid state. *Inorganica Chimica Acta*, 2, 202-207.
- Li, M.C., Judith, D., Liu, L. H., & Zhao, L. C. (2006). The phase transition and phase stability of magnetoelectric BiFeO₃. *Materials Science and Engineering A.*, 438-440, 346-349.
- Liu, Y. H., Li, J. B., Liang, J. K., Luo, J., Ji, L. N., Zhang, J. Y., & Rao, G. H. (2008) Phase diagram of the Bi₂O₃-Cr₂O₃ system. *Materials Chemistry and Physics*, 112, 239–243.
- Rico-Fuentes, O., Sanchez-Aguilera, E., Velasquez, C., Ortega-Alvarado, R., Alonso, J. C., & Ortiz, A. (2005). Characterization of spray deposited bismuth oxide thin films and their thermal conversion to bismuth silicate. *Thin Solid Films*, 478, 96– 102.
- Selbach, S. M., Tybell, T., Einarsrud, M-A., & Grande, T. (2010). Phase transitions, electrical conductivity and chemical stability of BiFeO₃ at high temperatures. *Journal of Solid State Chemistry*, 183, 1205-1208.
- Yang, C. H., Koo, T. Y., & Jeong, Y. H. (2007). Orbital order, magnetism, and ferroelectricity of multiferroic BiMnO₃. *Journal of Magnetism and Magnetic Materials*, 310, 1168–1170.

